The γWW Production in the Left-Right Symmetric Model

Aarre Pietilä[1]

and

Jukka Maalampi[2]

LR-report 5

Abstract

The production of the light W_1 and heavy W_2 weak gauge bosons in the reactions $e^-e^- \to \gamma W_1^- W_1^-, \gamma W_1^- W_2^-, \gamma W_2^- W_2^-$ has been investigated in the framework of the classic left-right symmetric electroweak model. These reactions arise due to the existence of Majorana neutrinos and doubly charged Higgs boson in the model. The final states $\gamma W_1^- W_1^-$ and $\gamma W_1^- W_2^-$ are only allowed through the mixings of the left- and right-handed bosons and the left- and right-handed neutrinos, and they are hence strongly suppressed.

The production of $\gamma W_2^- W_2^-$ is practically independent on the mixing angels. The cross section is roughly proportional to the square of the heavy neutrino mass m_2 and inversily proportional to the quartic of the mass M_{W_2} of W_2, except in the vicinity of the maximum of the cross section, where it decreases very quickly with the increasing M_{W_2}. We have applied a cut for the minimum energy E_{min} and for the minimum scattering angle θ_{min} of the photon. For example, taking $E_{min}/E_{cm} = 0.01$, $\cos\theta_{min} = 0.9$, $m_2 = 1$ TeV, $M_{W_2} = 0.5$ TeV, and 0.8 TeV for the mass of the Higgs Δ^{--}, we obtain about 28.3 fbarn for the maximum value of the cross section at 1.2 TeV. The cross sections can be greatly enhanced if the Higgs Δ^{--} lies at the neighbourhood of the collision energy. For example, keeping the other parameters same but setting $M_{\Delta^{--}} = 2$ TeV the cross section is 1.50 pbarn at the resonance. For a very heavy Δ^{--} ($M_{\Delta^{--}} \gtrsim 10$ TeV) our simple perturbational computation gives the value of 3 fbarn for the cross section at 2 TeV in the case of $M_{W_2} = 0.7$ TeV.

[1]Department of Applied Physics, University of Turku
[2]Department of Theoretical Physics, University of Helsinki

1 Introduction

The left-right (LR) symmetric electroweak model based on the gauge group $SU(2)_L \times SU(2)_R \times U(1)_{B-L}$ [1] has an important virtue of being able to explain the lightness of the neutrinos elegantly through the so-called see-saw mechanism [2]. The necessary incredients are the right-handed neutrinos (ν_R), and the $SU(2)_R$ triplet Higgses ($\Delta^{++}, \Delta^{+}, \Delta^{0}$) carrying two units of lepton number.

The LR-symmetry is broken into the standard model symmetry by a non-vanishing expectation value of Δ^0 at a scale $\gtrsim$ 1 TeV. The heavy gauge bosons $W_2(\simeq W_R + \zeta W_L)$ and Z_2, as well as the heavy Majorana neutrino $N(\simeq \nu_R + \eta\nu_L)$, achieve a mass proportional to $\langle\Delta^0\rangle$. The mixing parameters ζ and η are known to be small, at most of the order of 10^{-3}. The physical triplet Higgs particles, such as the doubly charged Δ^{++}, would have their masses in the same scale.

To obtain direct observational information about the new particles predicted by the LR-model, that is W_2, Z_2, the triplet Higgses, and the heavy neutrinos, one would need collision energies around 1 TeV or more. The next generation linear electron colliders [3] will provide an excellent environment for such a study as they are planned to operate in the energy range 0.5 to 2 TeV.

We have recently studied gauge boson production as a possible probe of the central predictions of the LR-model [4]. In particular, we have considered the lepton number violating processes $e^-e^- \to W^-W^-$ and $e^-e^- \to ZW^-W^-$ which give direct information about the mass of the Majorana neutrino and the double charged Higgs boson.

In [5], (to be called the Paper I in the following) we considered the reactions $e^-e^- \to ZW^-W^-$, where ZW^-W^- was allowed to be any combination of the ordinary charged weak boson W_1^-, the heavy charged weak boson W_2^-, and the light or heavy Z boson. In the present paper we shall investigate the related process where the Z boson is replaced by photon, i.e. $e^-e^- \to W^-W^-\gamma$. The formulas deduced in Paper I are valid in the photon case, except those depending on the polarization sum of the Z boson. This and the vanishing mass of the photon require, of course, some changes in the computational routines.

The reaction $e^-e^- \to \gamma W^-W^-$ has an advange, compared with the other processes $e^-e^- \to ZW^-W^-$, of having a lower production threshold and the increasement of the cross-section due to the soft photons. This may be important from phenomenological point of view since the total cross sections of the other processes have proved to be at best of the order of fbarn (without a Δ^{--} resonance). A general feature of the gauge boson processes we have considered has been that they are highly suppressed unless the W pair of the final state is W_2W_2. This is valid for $e^-e^- \to \gamma W^-W^-$, too, making the low threshold process $e^-e^- \to \gamma W_1^-W_2^-$ phenomenologically uninteresting.

We will reproduce in the following the relevant formulas of Paper I taking into account the modifications caused by the photon. After deriving the cross section for the process $e^-e^- \to \gamma W_2^-W_2^-$ we present numerical results for different choices of the unknown mass parameters and cuts for the photon energy and scattering angle.

2 Expressions for amplitudes and cross section

The lowest order Feynman graphs for the reaction $e^-e^- \to \gamma W_2^-W_2^-$ are presented in Fig 1. They are identical to the graphs of the process $e^-e^- \to ZW_2^-W_2^-$, which we considered in Paper I, except the diagram where the Z boson is produced in the virtual neutrino line.

The original left-right symmetric model with triplet Higgses would contain both one left-handed and one right-handed triplet. As the left-handed triplet has no dynamical role in the symmetry breaking we have omitted it in our considerations. As a consequence we have only one singly charged Higgs h^- in the unitary gauge. The diagrams containing this Higgs were neglected in Paper I, because they were estimated to produce a contribution, which is suppressed by the factor $M^2_{W_L}/M^2_{W_R}$. In the photon case the situation is even better. Those diagrams produce a contribution, which is proportional the coupling constant of $h\gamma W$, and this coupling vanishes exactly in the case of the photon.

For the amplitudes associated with the $W^-W^-\gamma$ production we can apply after appropriate modifications the expressions derived in Paper I for the $ZW_2^-W_2^-$ production. The relevant amplitudes are the following:

$$\begin{cases} T_1 = c \cdot \frac{\gamma^{\mu_1}\gamma^{\mu_2}(\not p_1 - \not k_3)\gamma^{\mu_3}}{(u_2 - m_2^2)\cdot t_{a3}}\ (1+\gamma_5), \\ T_2 = c \cdot \frac{\gamma^{\mu_3}(\not p_2 - \not k_3)\gamma^{\mu_1} g^{\mu_2}}{(u_1 - m_2^2)\cdot t_{b3}}\ (1+\gamma_5), \\ T_3 = c \cdot \frac{\gamma^{\mu_2}\gamma^{\mu_1}(\not p_1 - \not k_3)\gamma^{\mu_3}}{(t_2 - m_2^2)\cdot t_{a3}}\ (1+\gamma_5), \\ T_4 = c \cdot \frac{\gamma^{\mu_3}(\not p_2 - \not k_3)\gamma^{\mu_2} g^{\mu_1}}{(t_1 - m_2^2)\cdot t_{b3}}\ (1+\gamma_5), \end{cases} \tag{1}$$

$$\begin{cases} T_5 = -\,c\ \left[\frac{1}{t_2 - m_2^2} - \frac{1}{u_1 - m_2^2}\right] \cdot D^{W_2}_{\mu\nu}(k_1+k_3)\ F^{\mu_1\nu\mu_3}(k_1, k_1-k_3, k_3)\ \gamma^{\mu_2}\gamma^{\mu}\ (1+\gamma_5), \\ T_6 = -\,c\ \left[\frac{1}{u_2 - m_2^2} - \frac{1}{t_1 - m_2^2}\right] \cdot D^{W_2}_{\mu\nu}(k_2+k_3)\ F^{\mu_2\nu\mu_3}(k_2, k_2-k_3, k_3)\ \gamma^{\mu_1}\gamma^{\mu}\ (1+\gamma_5), \\ T_7 = -\,2c\ \left[\frac{1}{u_1 - m_2^2} + \frac{2}{s - M_\Delta^2}\right] \cdot D^{W_2}_{\mu\nu}(k_1+k_3)\ F^{\mu_1\nu\mu_3}(k_1, k_1-k_3, k_3)\ g^{\mu\mu_2}\ (1+\gamma_5), \\ T_8 = -\,2c\ \left[\frac{1}{t_1 - m_2^2} + \frac{2}{s - M_\Delta^2}\right] \cdot D^{W_2}_{\mu\nu}(k_2+k_3)\ F^{\mu_2\nu\mu_3}(k_2, k_2-k_3, k_3)\ g^{\mu\mu_1}\ (1+\gamma_5), \end{cases} \tag{2}$$

$$\begin{cases} T_9 = 4c \cdot \frac{g^{\mu_1\mu_2}}{s_3 - M_\Delta^2}\ \frac{\gamma^{\mu_3}(\not p_2 - \not k_3)}{t_{b3}}\ (1+\gamma_5), \\ T_{10} = 4c \cdot \frac{g^{\mu_1\mu_2}}{s_3 - M_\Delta^2}\ \frac{(\not p_1 - \not k_3)\gamma^{\mu_3}}{t_{a3}}\ (1+\gamma_5), \\ T_{11} = 16c \cdot \frac{g^{\mu_1\mu_2}}{s_3 - M_\Delta^2}\ \frac{(p_1+p_2)^{\mu_3}}{s - M_\Delta^2}\ (1+\gamma_5). \end{cases} \tag{3}$$

where

$$c = -m_2\ e\ g_R^2/4. \tag{4}$$

The total reaction amplitude T is a sum of the partial amplitudes T_i. The variables s_1, s_2, s_3, t_1, t_2, u_1, u_2, t_{a3}, and t_{b3} are defined by

$$\begin{cases} s = (p_1+p_2)^2, \\ s_1 = (k_1+k_3)^2, \\ s_2 = (k_2+k_3)^2, \\ t_1 = (p_1-k_1)^2, \\ t_2 = (p_2-k_2)^2, \\ u_1 = (p_1-k_2)^2 = s_1 - t_2 - s + M_2^2, \\ u_2 = (p_2-k_1)^2 = s_2 - t_1 - s + M_1^2, \\ s_3 = (k_1+k_2)^2 = s - s_1 - s_2 + M_1^2 + M_2^2 + M_3^2, \\ t_{a3} = (p_1-k_3)^2 = t_2 - t_1 - s_1 + M_1^2 + M_3^2, \\ t_{b3} = (p_2-k_3)^2 = t_1 - t_2 - s_2 + M_2^2 + M_3^2. \end{cases} \tag{5}$$

The relative signs of the different amplitudes T_i are, of course, of great importance in order the cancellations that guarantee the good high energy behaviour to work. In Paper I we checked the signs by using subprocesses. If one drops in the the amplitudes 5 and 7 arising from the diagrams b and c the common tail where a virtual W-boson decays into a ZW pair, we have a subprocess $e^-e^- \to W\ W(2)$, a process we have considered previously [4]. The amplitudes 6 and 8 form a similar pair. Similarly one can consider the amplitudes 9, 10 and 11, related to the diagrams d and e of Fig 3. If one drops the tail where Δ decays into a W-pair, one has the subprocess $e^-e^- \to Z\ \Delta^{--}$. It contains three amplitudes, one in t-channel, one in u-channel, and one in

s-channel, which have to balance each other in order to get a good high-energy behaviour of the total cross section.

In our present case the gauge invariance provides an even better check of the relative signs of the subamplitudes. The complete scattering amplitude is of the form

$$M = i^5 \overline{v}(e_2)\, T^{\mu_1\mu_2\mu_3} u(e_1)\, \varepsilon^*_{\mu_1}(W_{l_1})\, \varepsilon^*_{\mu_2}(W_{l_2})\, \varepsilon^*_{\mu_3}(\gamma). \tag{6}$$

The gauge invariance is guaranteed if the replacement of $\varepsilon^*_{\mu_3}(\gamma)$ by $k_3^{\mu_3}$ would make M to vanish. It is easy to convince oneself about this by making usual spinor manipulations and by taking into account that in our expressions we have neglected the electron mass.

After a squaring and spin summation (6) leads to

$$\sum_{spins} |M|^2 = -(g^{\mu_1\nu_1} - \frac{k_1^{\mu_1} k_1^{\nu_1}}{M_1^2})\,(g^{\mu_2\nu_2} - \frac{k_2^{\mu_2} k_2^{\nu_2}}{M_2^2})\,(g^{\mu_3\nu_3}) \cdot \mathrm{Tr}\,\{T_{\mu_1\mu_2\mu_3}\, \not{p}_1 \gamma^0 (T_{\nu_1\nu_2\nu_3})^\dagger \gamma^0\, \not{p}_2\}. \tag{7}$$

Here we have used the fact that the quantity, obtained from the complete amplitude M by dropping $\varepsilon^*_{\mu_3}(\gamma)$, is orthogonal to the momentum of the photon, which simplifies the sum over the polarizations of the transversal photons to $-g^{\mu_3\nu_3}$.

The total cross section of the production of the unpolarized final state γWW in a collision of unpolarized electrons is then given by the formula

$$\sigma_3 = \frac{1}{(2\pi)^5} \frac{\int \prod_{i=1}^3 \frac{d^3 k_i}{2E_i} \delta^4(p_1 + p_2 - \sum k_i) \langle \Sigma |M|^2 \rangle}{2s} \tag{8}$$

with

$$\langle \Sigma |M|^2 \rangle = \frac{1}{4} \sum_{spins} |M|^2. \tag{9}$$

The expression (8) should be devided by two in the case of two identical bosons in the final state. Furthermore, in order to get a finite result the phase space integration must be restricted so that the photons scattering along the beam axis or having vanishing momenta are cut out.

Our formulas for the amplitudes have been given in the case where the width of Δ^{--} can be neglected. The finite width of Δ, however, does not remarkably complicate our computation. The width of Δ can be evaluated by using the formulas

$$\begin{aligned}
\Gamma_{\Delta^{--}\to l^- l^-} &= \frac{g_R^2 M_\Delta}{32\pi} \frac{M_{\nu_e}^2 + M_{\nu_\mu}^2 + M_{\nu_\tau}^2}{M_{W_2}^2}, \\
\Gamma_{\Delta^{--}\to W_2^- W_2^-} &= \frac{g_R^2 M_\Delta}{4\pi} \sqrt{1 - 4(\frac{M_{W_2}}{M_\Delta})^2}\, [1 - (\frac{M_{W_1}}{M_{W_2}})^2]\, [3(\frac{M_{W_2}}{M_\Delta})^2 + \tfrac{1}{4}(\frac{M_\Delta}{M_{W_2}})^2 - 1], \\
\Gamma_{\Delta^{--}\to W_2^- h^-} &= \frac{g_R^2 M_\Delta}{4\pi} (\frac{M_{W_1} M_\Delta}{M_{W_2}^2})^2\, \lambda^{3/2}[1, (\frac{M_{W_2}}{M_\Delta})^2, (\frac{M_h}{M_\Delta})^2]\,.
\end{aligned} \tag{10}$$

The two first formulas (for the left-handed triplet) can be found in the paper of Gunion et al [6]. This reference also gives an equation from which the third formula can be deduced when Δ^- is expressed as a linear combination of the mass eigen state h^- and a Goldstone. In order to reduce our parameter set, we have assumed h so heavy that the third channel can be dropped in the width of Δ^{--}.

3 Numerical results and discussion

The computation has been performed by using the symbolic manipulation programs REDUCE and Mathematica and the Monte Carlo integration rutine Vegas (see Paper I for details). The only new feature comparing with the WWZ case is the handling of the soft-photon singularity. In most

new feature comparing with the WWZ case is the handling of the soft-photon singularity. In most cases the singularity has been evaded by using cuts for the minimum energy and the minimum scattering angle of the photon. We also used the transversal momentum cut of the photon alone.

For the mass of the heavy W-boson we used values 0.5 - 0.7 TeV, which are near to the experimental lower bound. The mass of Δ^{--} Higgs was varied in broad limits from 0.8 TeV up to 10 TeV.

The cross section is proportional to the square of the mass of the heavy neutrino for which we use the value $M_\nu = 1$ TeV. In fact, the cosmological lower bound of M_ν is about 3 GeV and the TeV region is not at all unnatural. At the energies considerably above the neutrino mass the cross section roughly scales with M_ν^2.

The total amplitude consists of the partial amplitudes coming from the different diagrams and from the permutations of the final particles in them. We have used here two partitions. The first one corresponds to the decomposition given by (1) - (3) and is based on the subprocesses as described earlier. In spite of the clear physical basis, the contributions from the different parts of this partition are unphysical, because we have applied a formula of the transversal photon polarization sum which is correct in the case of the total amplitude but incorrect if it would be applied for these partial amplitudes. In the other partition the channels mediated by the neutrinos are separated from the channels having virtual Δ^{--} Higgses. The contributions from the both parts now are physical, because the amplitude sets corresponding to this partition are orthogonal to the momentum of the photon just like the total amplitude.

In Fig. 2 we present the contributions of various subprocess sets to the total cross section in the energy region of 1 - 5 TeV using parameter values $M_{W_2} = 0.5$ TeV, $M_{\nu_2} = 1.0$ TeV and $M_\Delta = 0.8$ TeV. (The low value of M_Δ allows us to study the high-energy behavior of the cross section without Δ-pole complications.) The sets have been enumerated by the indices corresponding to the amplitudes involved. The amplitudes $T_5 + T_7$ and $T_6 + T_8$, which both corresponds to the subprocess $e^-e^- \to W_2^- W_2^-$ with one decaying W, have been summed and they lead to the contribution $\sigma_{(5-8)\times(5-8)}$. (The negative value of this contribution is a consequence of the fact that the contributions involved do not close the photon polarization sum.) We note that the fan-like structure of the various contributions typical for the $e^-e^- \to W^-W^-Z$ is not visible here. The Fig. 3 presents the division of the cross section into the neutrino and Higgs contributions. These both parts are now physical their separate contributions being positive, and their interference contribution is negative as necessary for a good high energy behaviour.

In Fig. 4 we present the total cross section for three sets of the photon energy and scattering angle cuts.

To demonstrate the good high-energy behaviour of the cross section we show in in Fig. 5 the cross section as a function of the center of mass energy up to 20 TeV. (We have checked the monotonical decrease of the cross section up to the energy 800 TeV.) Fig. 6 presents the cross section as a function of energy for a slightly heavier W_2 ($M_{W_2} = 0.7$ TeV). One should note the large decrease of the maximum value of the cross section, to some 20th part of its previous value. With the increasing energy the cross section approaches to the value expected according to the scaling with the W_2 mass at high energies. We note that the finite width of Δ does not essentially change the results presented in Figs. 2-6, because the main open channel of Δ is into two leptons and this is still quite narrow for the Δ^{--} mass of 0.8 TeV.

Fig. 7 is the same as Fig. 2 but the mass of Δ^{--} being 10 TeV. The different contributions now form a fan-like picture where the cancellations among the various terms are easy to visualize. Fig. 8 presents the other partition of the total cross section for the same Higgs mass. The cross section presented in these figures have been calculated without taking into account the width of Δ^{--} Higgs. In fact, for so high a mass the channel $\Delta^{--} \to W_2^- \; W_2^-$ alone gives rise to a width which is greater than the mass of the Higgs. If we still simple minded apply our perturbational computation and use such a huge width we get the result which at the energy of 2 TeV can be read from the curve $\sigma_{n\times n}$ of the pure neutrino contribution in Fig. 8.

Fig. 9 shows the total cross section for the other cut parameters of the photon energy and scattering angle and Fig. 10 presents corresponding results in the case $M_{W_2} = 0.7$ TeV.

In Fig. 11 we present the total cross section for two sets of the photon cuts assuming a Δ-pole at 2 TeV with a width of $\Gamma = 0.14 M_\Delta$.

In summary, we have calculated the total cross section for the production of a heavy W_2 pair along with a photon using different choises for the unknown mass parameters and different cuts for the photon energy and scattering angles. If the mass of the heavy electron neutrino is of order of 1 TeV and the W_2 mass near to 0.5 TeV, the cross section in the energy region of few TeV is in the range of 1 - 10 fbarn. It can reach the value 1 pbarn in the case of a Δ^{--} resonance. As compared with the production rate of a heavy W_2 pair alone this process yields a background of order of 1 % for reasonable scattering angle cuts.

Acknowledgements

The authors thank Mr. Juha Vuori for his help in numerical work. The work has been financially supported by Turun yliopistosäätiö and the Academy of Finland.

References

[1] J.C. Pati and A. Salam, Phys. Rev. D10, 275 (1974); R.N. Mohapatra and J.C. Pati, Phys. Rev. D11, 566, 2558 (1975); G. Senjanovic, Nucl. Phys. B153, 334 (1979).

[2] M. Gell-Mann, P. Ramond and R. Slansky, in *Supergravity*, eds. P. van Niewenhuizen and D. Z. Freedman (North Holland 1979);
T. Yanagida, in Proceedings of *Workshop on Unified Theory and Baryon Number in the Universe*, eds. O. Sawada and A. Sugamoto (KEK 1979).

[3] B. Wiik, a talk in the *Workshop on physics and experiments with linear colliders* (Saariselkä, Finland, September 1991), eds. R. Orava, P. Eerola and M. Nordberg (World Scientific, 1992), p. 83.

[4] J. Maalampi, A. Pietilä and J. Vuori, Nucl. Phys. B 381 (1992) 544, and Phys. Lett. B 297 (1992) 327;
J. Maalampi and A. Pietilä, Z. Phys. C59 (1993) 257;
J. Maalampi, A. Pietilä and M. Raidal, Phys. Rev. D 48 (1993) 4467; A. Pietilä, J. Maalampi, and J. Vuori, Laboratory report Turku-FL-R9, Department of Physics, University of Turku, Finland (1992).

[5] A. Pietilä and J. Maalampi, Laboratory report Turku-SFL-R9, Department of Applied Physics, University of Turku, Finland (1993).

[6] N.G. Deshpande, J.F. Gunion, B. Kayser, and F. Olness, Phys. Rev. D44. 837 (1991); J.F. Gunion, J. Grifos, A. Mendes, B. Kayser, and F. Olness, Phys. Rev. D40, 1546 (1989).

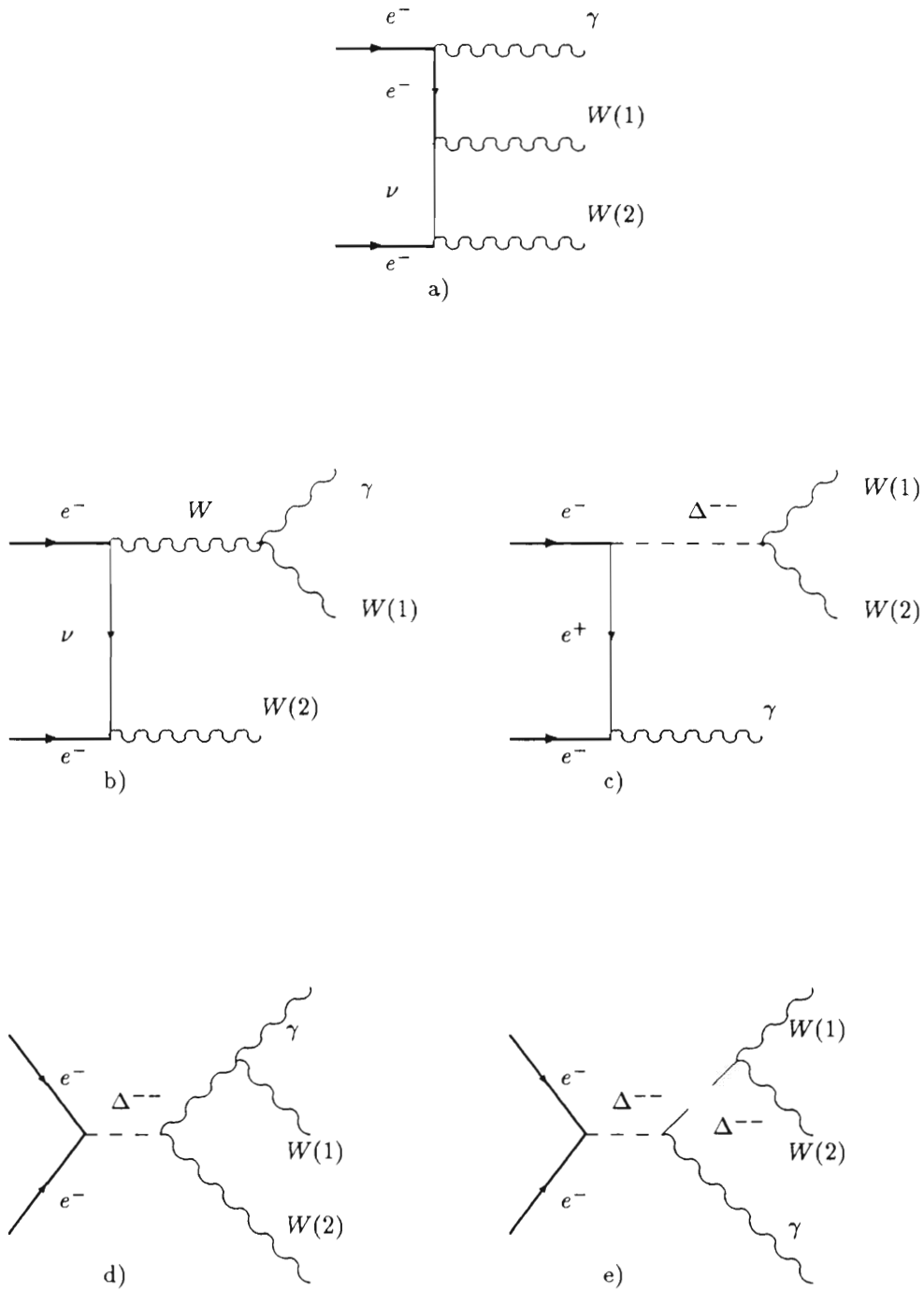

Figure 1: The lowest-order Feynman graphs for the process $ee \to \gamma WW$

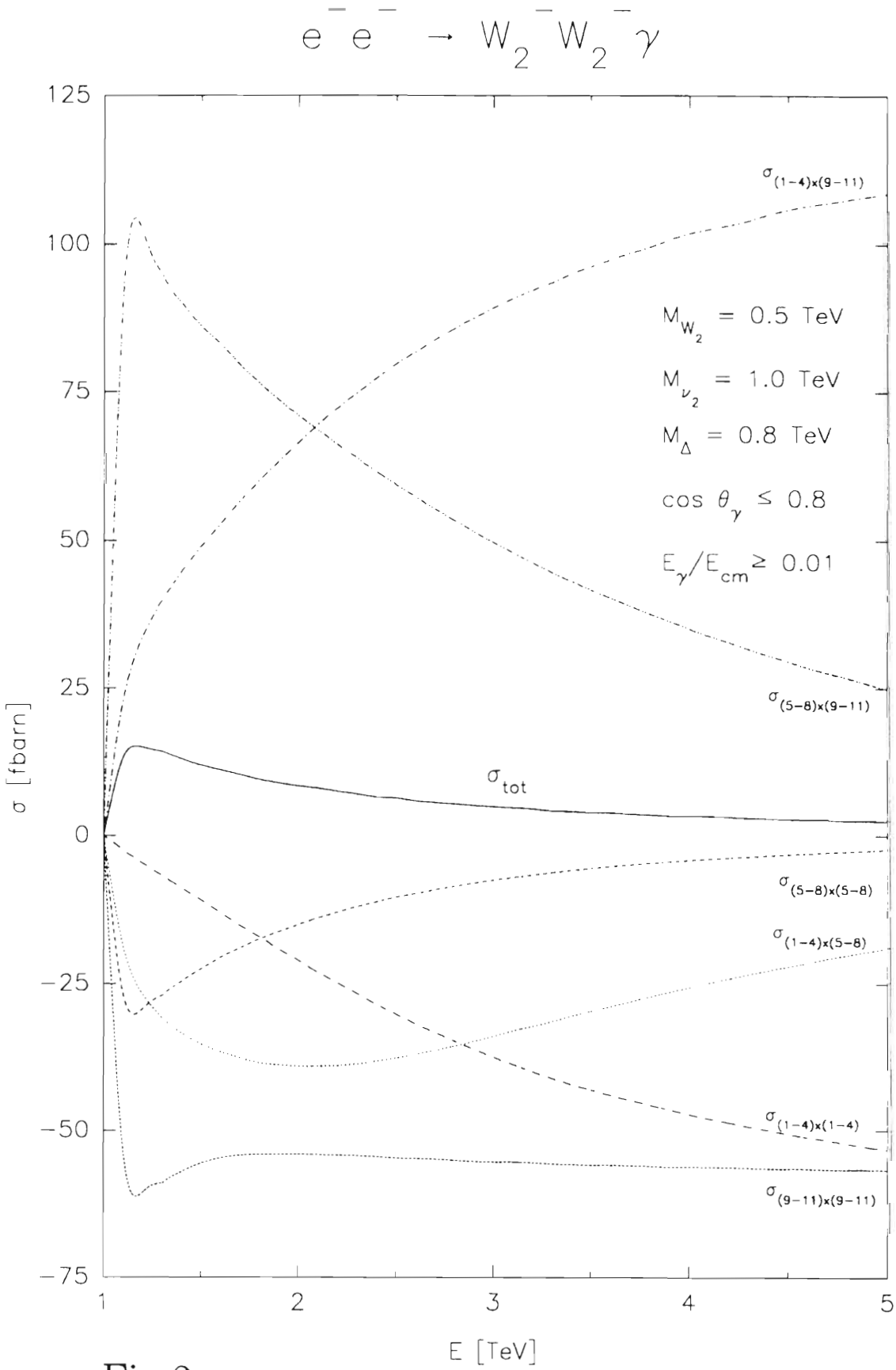
$e^- e^- \to W_2^- W_2^- \gamma$
125
100
75
50
25
0
−25
−50
−75
1
2
3
4
5
σ [fbarn]
E [TeV]
$\sigma_{(1-4)\times(9-11)}$
M_{W_2} = 0.5 TeV
M_{ν_2} = 1.0 TeV
M_Δ = 0.8 TeV
cos $\theta_\gamma \leq 0.8$
$E_\gamma/E_{cm} \geq 0.01$
$\sigma_{(5-8)\times(9-11)}$
σ_{tot}
$\sigma_{(5-8)\times(5-8)}$
$\sigma_{(1-4)\times(5-8)}$
$\sigma_{(1-4)\times(1-4)}$
$\sigma_{(9-11)\times(9-11)}$

Fig 2

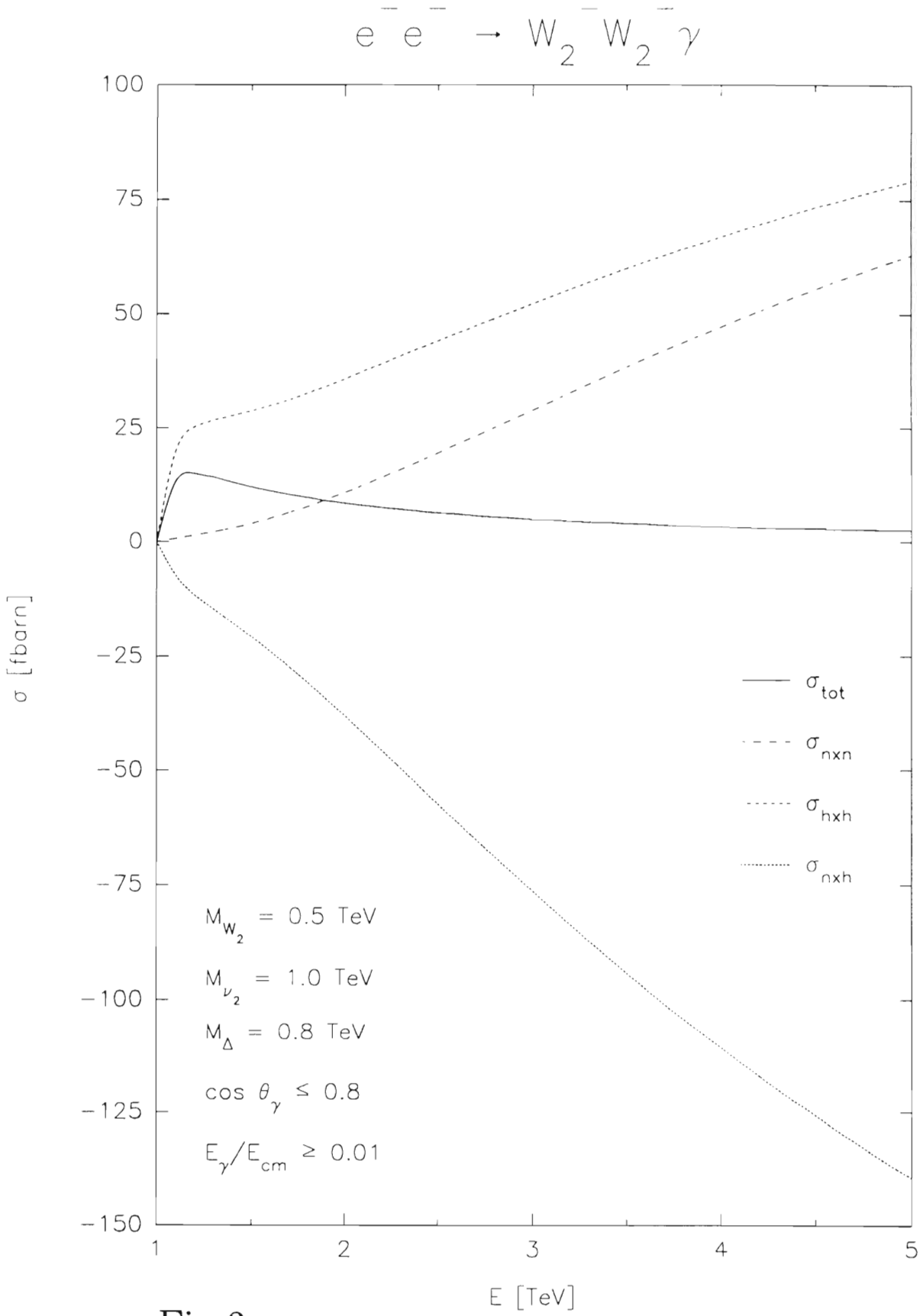
$e^- e^- \to W_2^- W_2^- \gamma$
100
75
50
25
0
−25
−50
−75
−100
−125
−150
σ [fbarn]
1
2
3
4
5
E [TeV]
σ_{tot}
σ_{nxn}
σ_{hxh}
σ_{nxh}
M_{W_2} = 0.5 TeV
M_{ν_2} = 1.0 TeV
M_Δ = 0.8 TeV
$\cos\theta_\gamma \leq 0.8$
$E_\gamma/E_{cm} \geq 0.01$

Fig 3

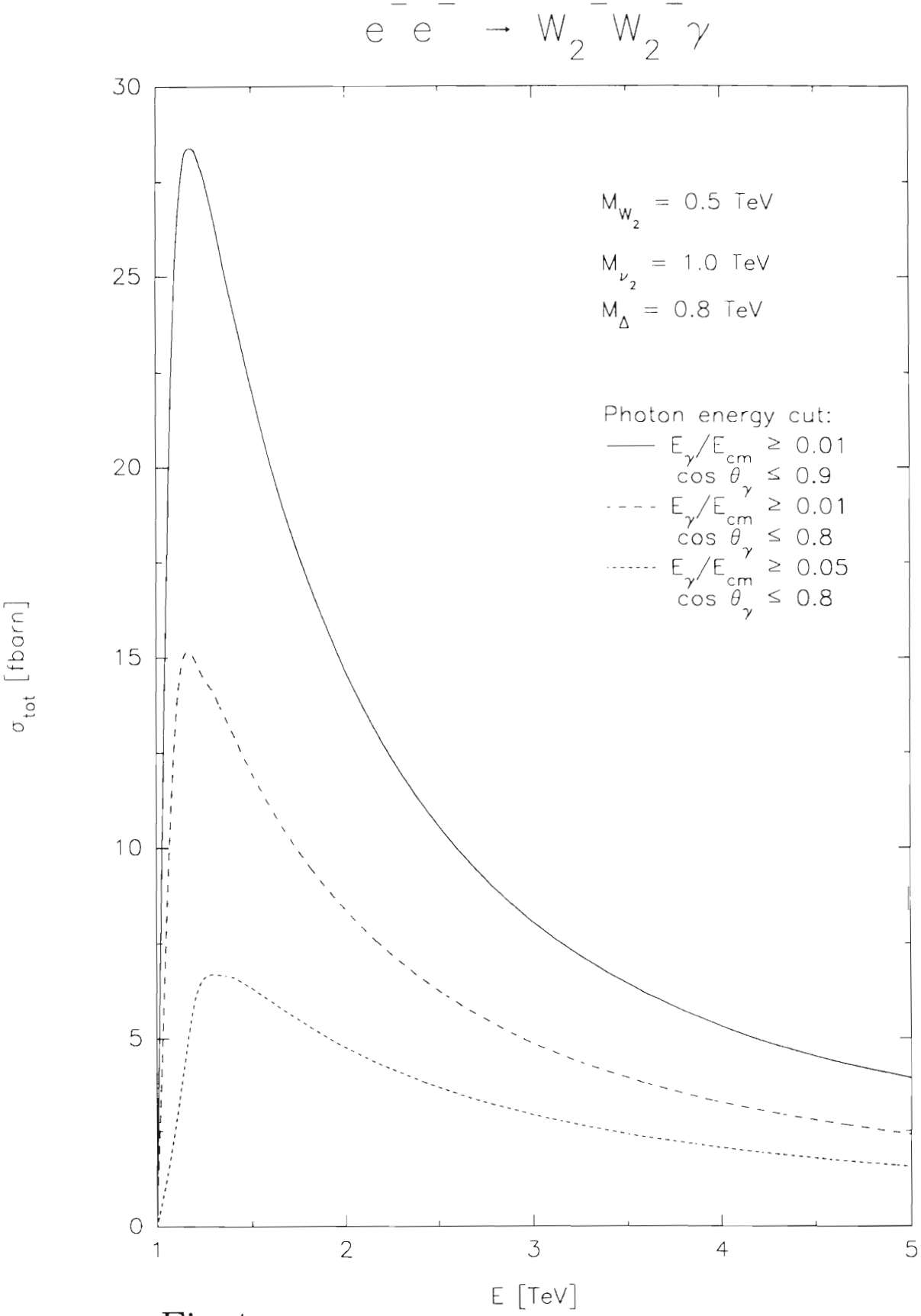
$e^- e^- \to W_2^- W_2^- \gamma$
M_{W_2} = 0.5 TeV
M_{ν_2} = 1.0 TeV
M_Δ = 0.8 TeV
Photon energy cut:
$E_\gamma/E_{cm} \geq 0.01$
$\cos\theta_\gamma \leq 0.9$
$E_\gamma/E_{cm} \geq 0.01$
$\cos\theta_\gamma \leq 0.8$
$E_\gamma/E_{cm} \geq 0.05$
$\cos\theta_\gamma \leq 0.8$
σ_{tot} [fbarn]
E [TeV]
0
5
10
15
20
25
30
1
2
3
4
5

Fig 4

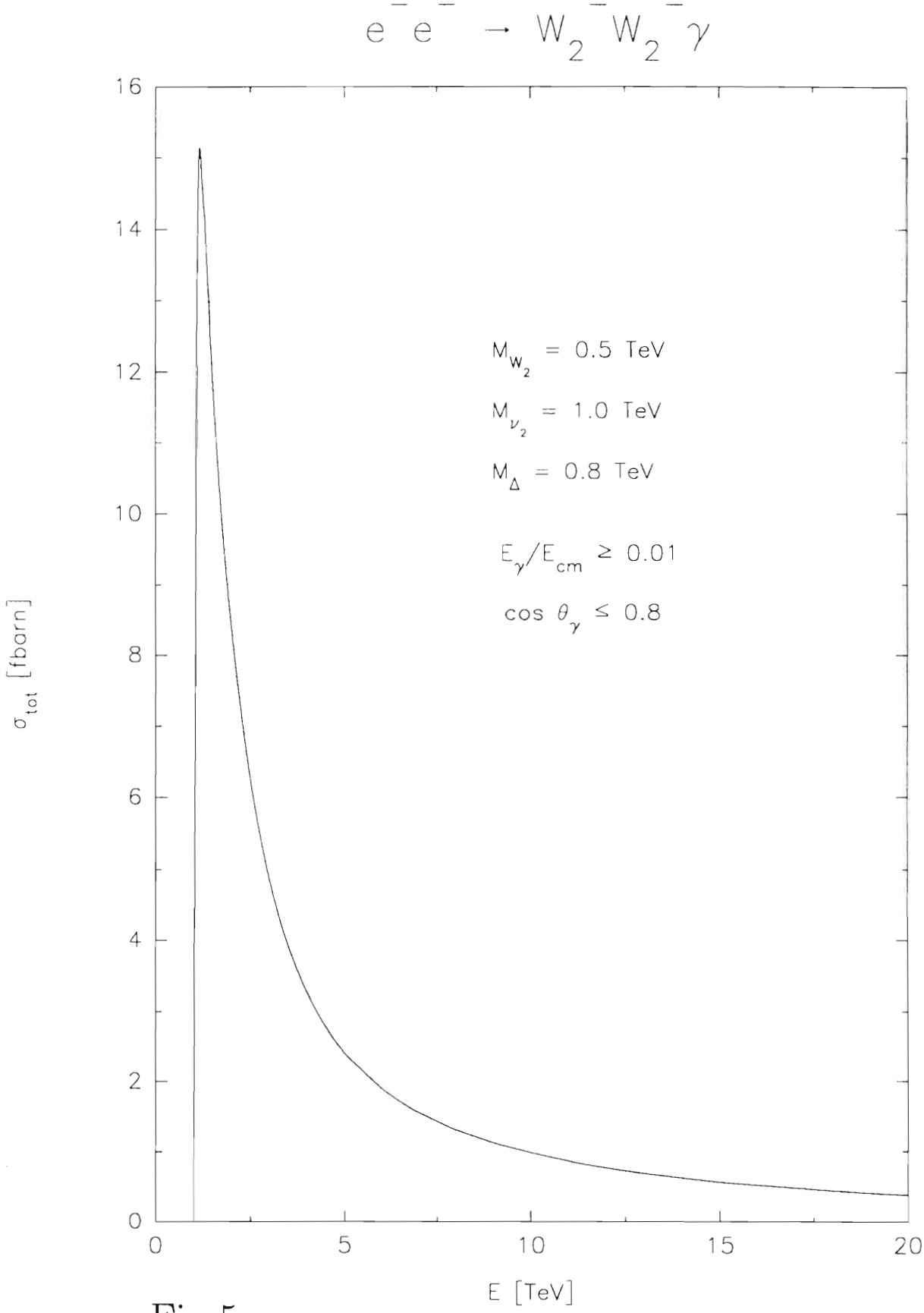
$e^- e^- \to W_2^- W_2^- \gamma$
M_{W_2} = 0.5 TeV
M_{ν_2} = 1.0 TeV
M_Δ = 0.8 TeV
$E_\gamma/E_{cm} \geq 0.01$
$\cos\theta_\gamma \leq 0.8$
σ_{tot} [fbarn]
E [TeV]
0
2
4
6
8
10
12
14
16
0
5
10
15
20

Fig 5

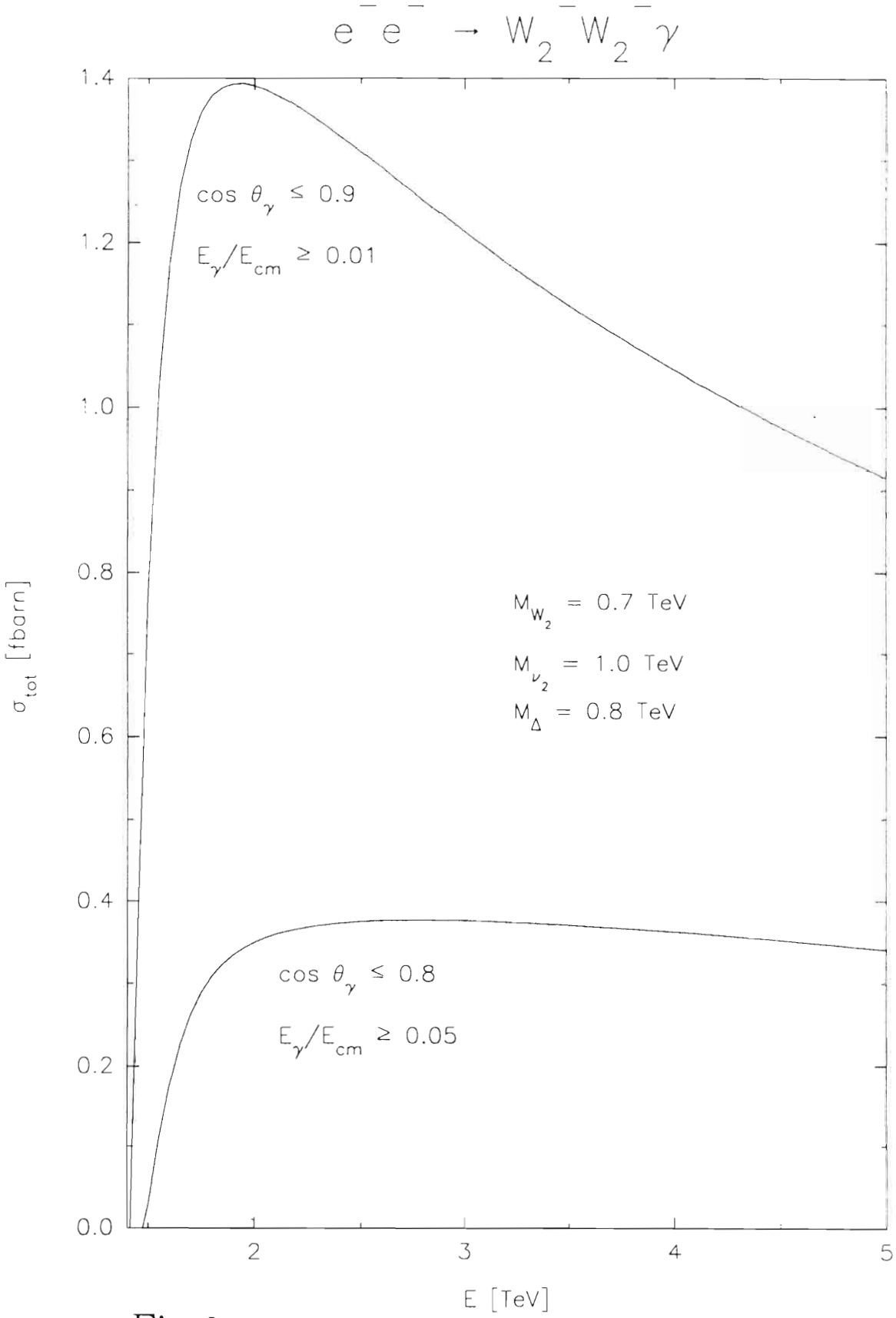
$e^- e^- \to W_2^- W_2^- \gamma$
1.4
1.2
1.0
0.8
0.6
0.4
0.2
0.0
σ_{tot} [fbarn]
$\cos\theta_\gamma \le 0.9$
$E_\gamma/E_{cm} \ge 0.01$
$M_{W_2} = 0.7$ TeV
$M_{\nu_2} = 1.0$ TeV
$M_\Delta = 0.8$ TeV
$\cos\theta_\gamma \le 0.8$
$E_\gamma/E_{cm} \ge 0.05$
2
3
4
5
E [TeV]

Fig 6

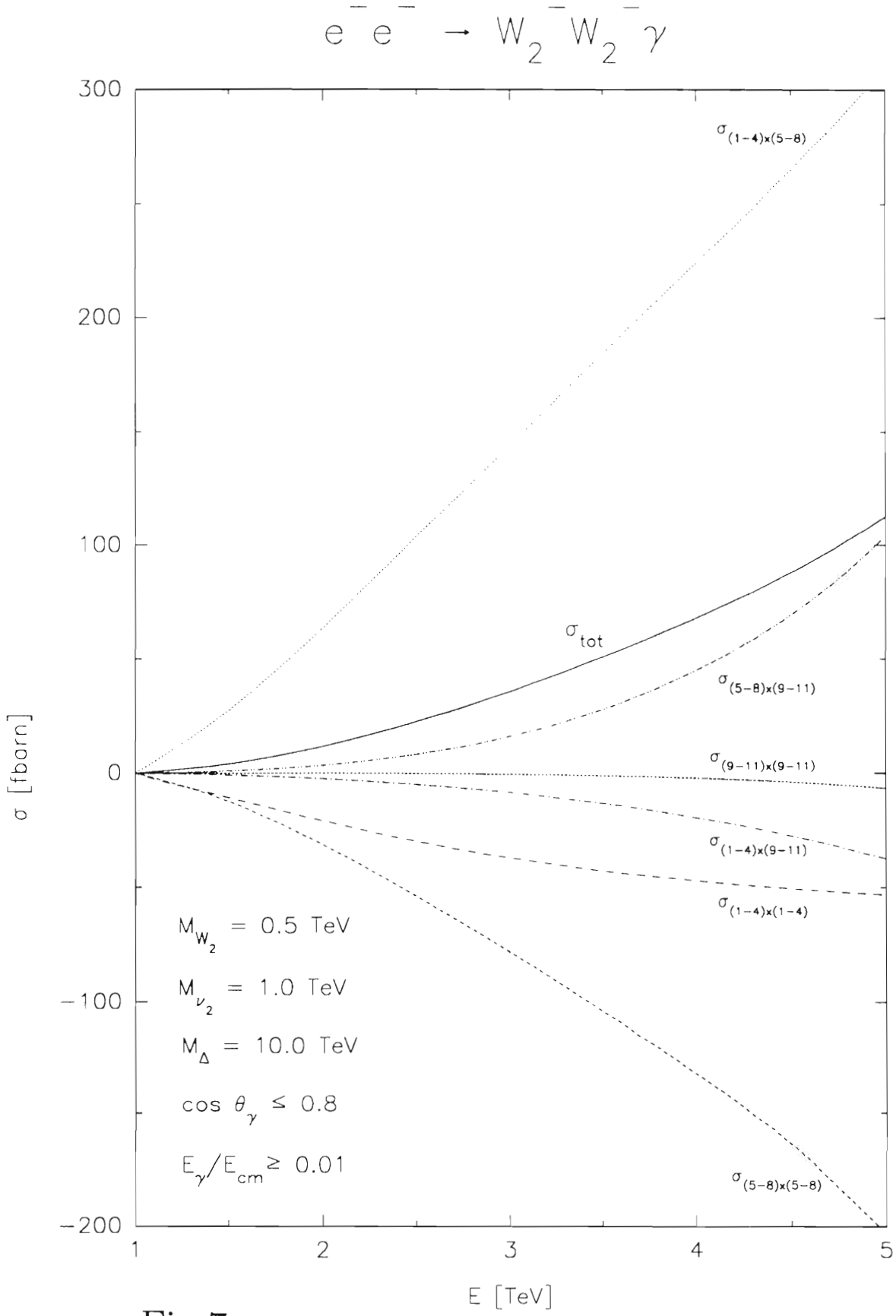
$e^- e^- \to W_2^- W_2^- \gamma$
300
200
100
0
−100
−200
σ [fbarn]
1
2
3
4
5
E [TeV]
$\sigma_{(1-4)\times(5-8)}$
σ_{tot}
$\sigma_{(5-8)\times(9-11)}$
$\sigma_{(9-11)\times(9-11)}$
$\sigma_{(1-4)\times(9-11)}$
$\sigma_{(1-4)\times(1-4)}$
$\sigma_{(5-8)\times(5-8)}$
M_{W_2} = 0.5 TeV
M_{ν_2} = 1.0 TeV
M_Δ = 10.0 TeV
$\cos\theta_\gamma \leq 0.8$
$E_\gamma/E_{cm} \geq 0.01$

Fig 7

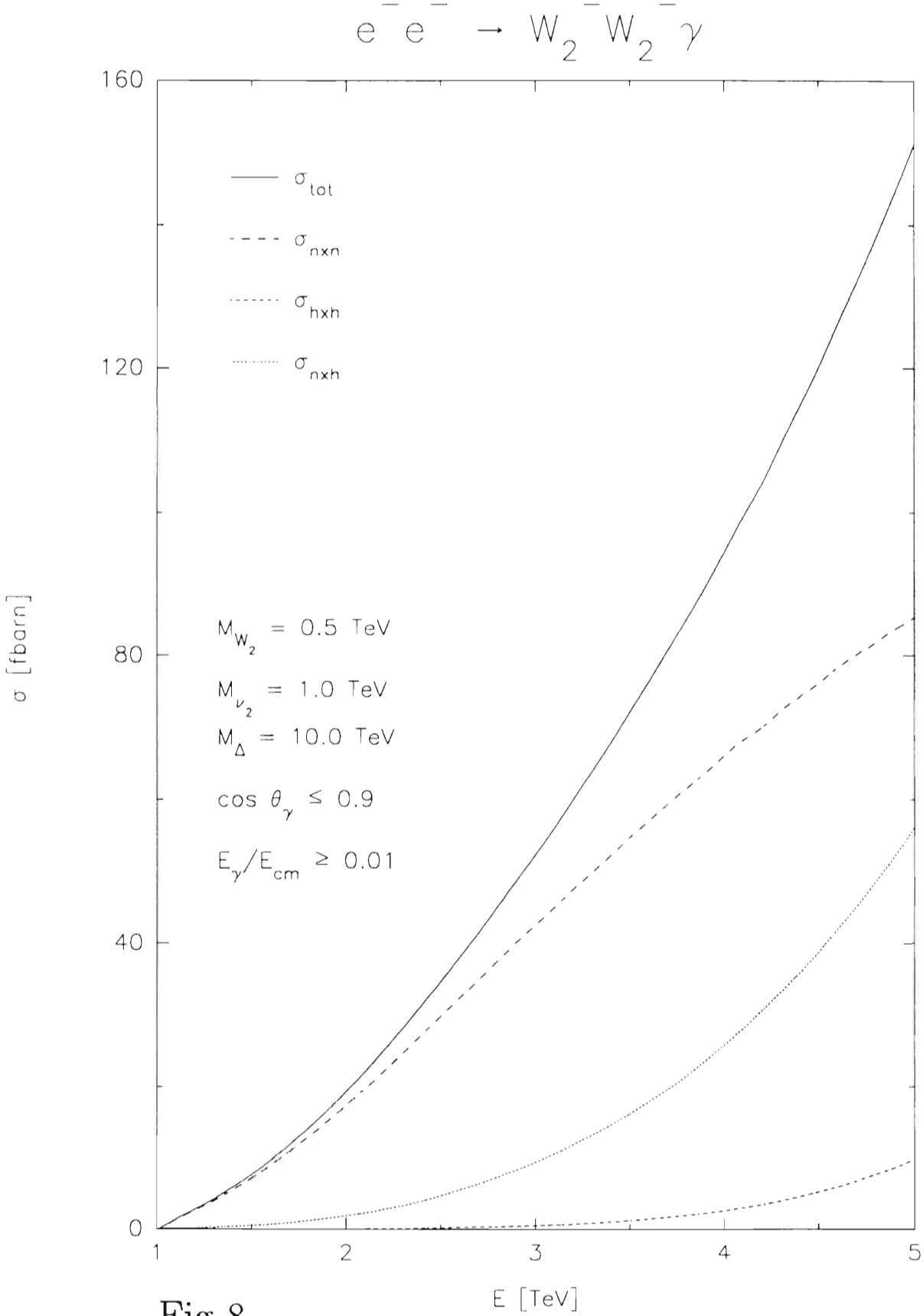
$e^- e^- \to W_2^- W_2^- \gamma$
160
120
80
40
0
1
2
3
4
5
σ [fbarn]
E [TeV]
σ_{tot}
σ_{nxn}
σ_{hxh}
σ_{nxh}
M_{W_2} = 0.5 TeV
M_{ν_2} = 1.0 TeV
M_Δ = 10.0 TeV
$\cos\theta_\gamma \leq 0.9$
$E_\gamma/E_{cm} \geq 0.01$

Fig 8

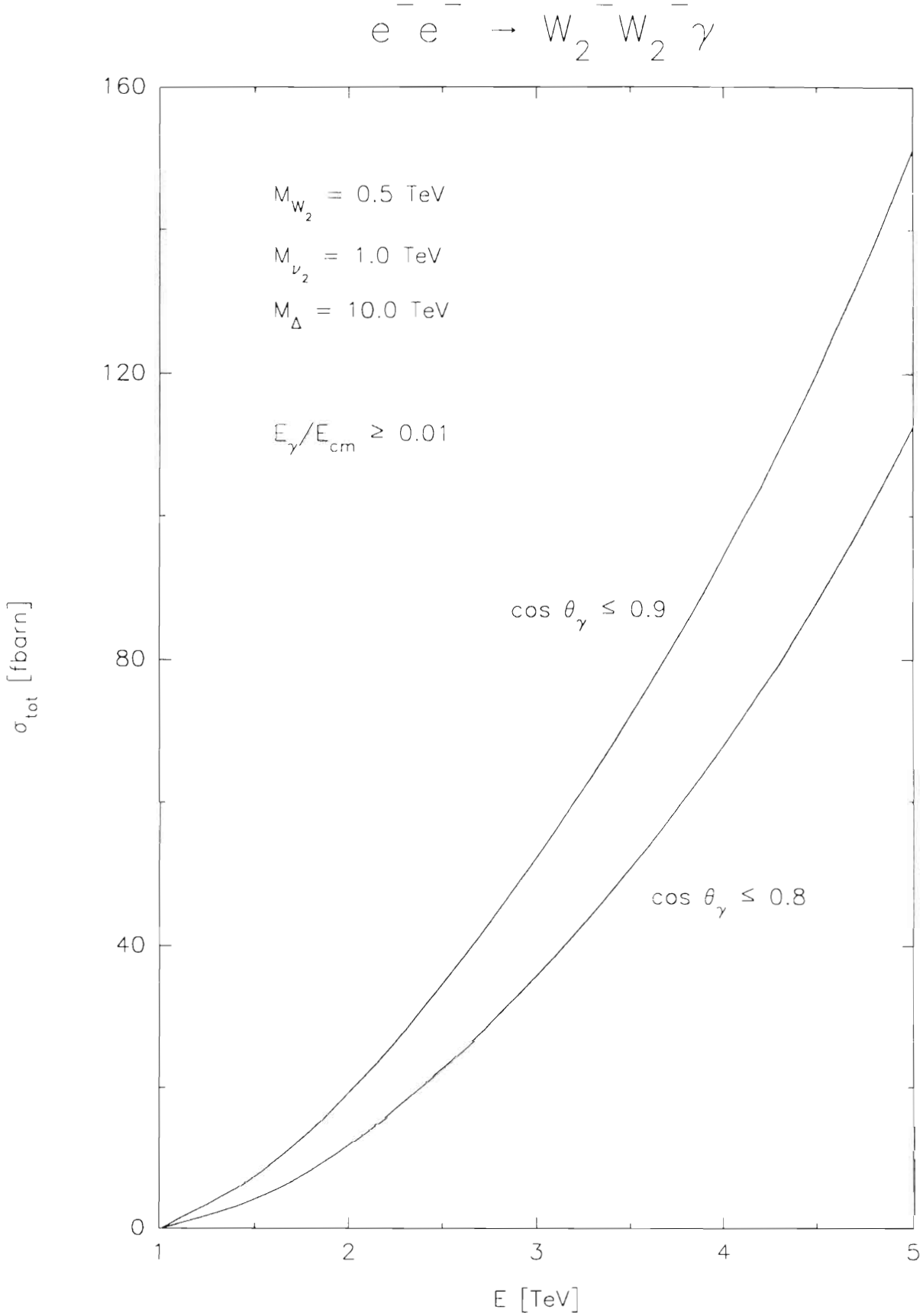
$e^- e^- \to W_2^- W_2^- \gamma$
M_{W_2} = 0.5 TeV
M_{ν_2} = 1.0 TeV
M_Δ = 10.0 TeV
$E_\gamma/E_{cm} \geq 0.01$
$\cos\theta_\gamma \leq 0.9$
$\cos\theta_\gamma \leq 0.8$
σ_{tot} [fbarn]
E [TeV]
0
40
80
120
160
1
2
3
4
5

Fig 9

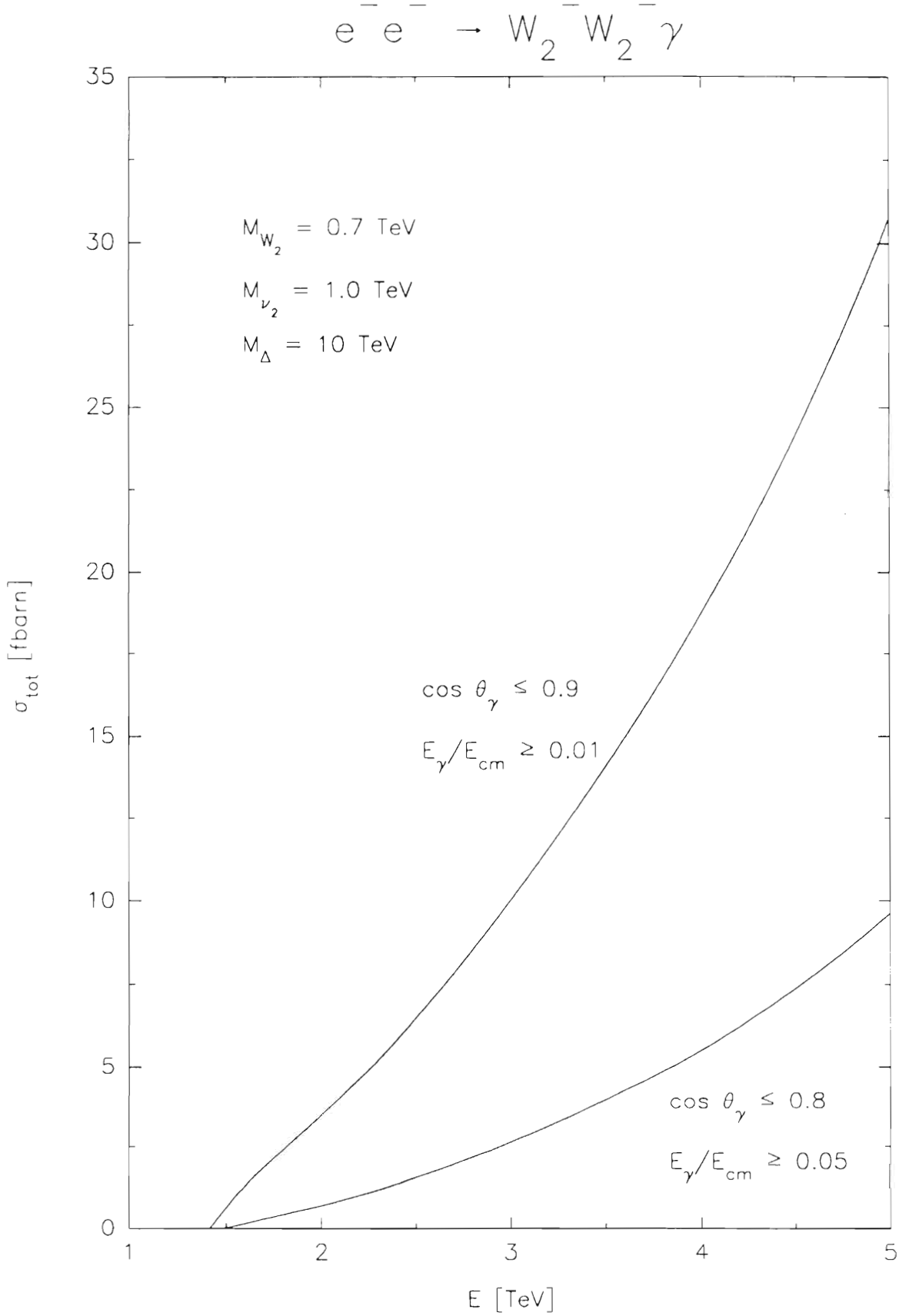
$e^- e^- \to W_2^- W_2^- \gamma$
M_{W_2} = 0.7 TeV
M_{ν_2} = 1.0 TeV
M_Δ = 10 TeV
$\cos\theta_\gamma \leq 0.9$
$E_\gamma/E_{cm} \geq 0.01$
$\cos\theta_\gamma \leq 0.8$
$E_\gamma/E_{cm} \geq 0.05$
σ_{tot} [fbarn]
E [TeV]
0
5
10
15
20
25
30
35
1
2
3
4
5

Fig 10

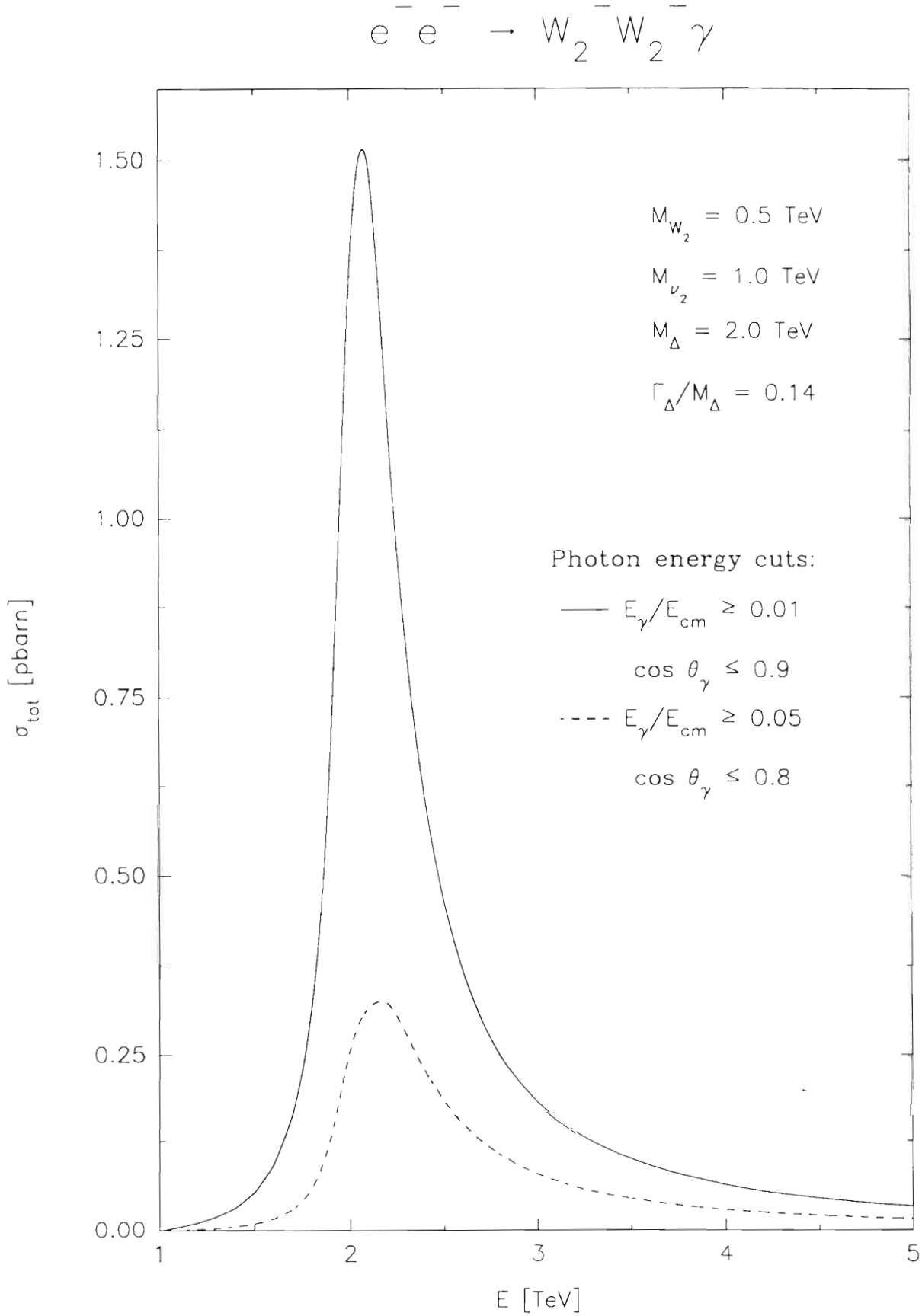
$e^- e^- \to W_2^- W_2^- \gamma$
M_{W_2} = 0.5 TeV
M_{ν_2} = 1.0 TeV
M_Δ = 2.0 TeV
Γ_Δ/M_Δ = 0.14
Photon energy cuts:
$E_\gamma/E_{cm} \geq 0.01$
$\cos\theta_\gamma \leq 0.9$
$E_\gamma/E_{cm} \geq 0.05$
$\cos\theta_\gamma \leq 0.8$
σ_{tot} [pbarn]
E [TeV]
1.50
1.25
1.00
0.75
0.50
0.25
0.00
1
2
3
4
5

Fig 11